Published in final edited form as:
Ultrasound Med Biol. 2012 April ; 38(4): 670–680. doi:10.1016/j.ultrasmedbio.2011.12.025.

ULTRASONIC IMAGING OF ENDOTHELIAL CD81 EXPRESSION USING CD81-TARGETED CONTRAST AGENTS IN *IN VITRO* AND *IN VIVO* STUDIES

Fei Yan[*], **Xiang Li**[*], **Qiaofeng Jin**[*], **Juanjuan Chen**[*], **Robin Shandas**[†], **Junru Wu**[‡], **Lu Li**[*], **Tao Ling**[*], **Wei Yang**[*], **Yun Chen**[§], **Xin Liu**[*], and **Hairong Zheng**[*]

[*]Paul C. Lauterbur Research Center for Biomedical Imaging, Institute of biomedical and Health Engineering, Shenzhen Institutes of Advanced Technology, Chinese Academy of Sciences, Shenzhen, China

[†]Department of Mechanical Engineering, University of Colorado, Boulder, CO, USA

[‡]Department of Physics, University of Vermont, Burlington, VT, USA

[§]Department of Ultrasonography, Shenzhen Hospital of Peingking University, Shenzhen, China

Abstract

This study is designed to investigate the feasibility for molecular imaging of endothelial CD81 expression *in vitro* and *in vivo* using the CD81-targeted ultrasound contrast agents (UCA). In the *in vitro* study, murine bEnd.3 cells were stimulated with phenazine methosulfate (PMS), an oxidative stress inducer. Changes in CD81 expression after stimulation were confirmed by Western blotting, tracked by using the targeted UCA and further imaged under ultrasound imaging system with 5 MHz transmit frequency. In the *in vivo* study, expression of endothelial CD81 proteins in murine carotid artery vessels was studied using high-frequency ultrasound system with 40 MHz transmit frequency. Our results showed that endothelial CD81 expression was gradually up-regulated with the increase of PMS concentration. Correspondingly, the accumulation of targeted UCA was gradually improved and could be inhibited significantly upon addition of free anti-CD81 antibodies. The mean video intensity (grey-level) of stimulated cells and vessels from backscatter of the CD81-targeted UCA was 17.2 (interquartile range [IQR] 15.4–19.8) and 27.2 (IQR 22.4–29.8), significantly greater than that of non-stimulated cells with 9.0 (IQR 8.6–10.8) ($p < 0.01$) and non-stimulated vessels with 11.3 (IQR 10.4–13.2) ($p < 0.01$), respectively. In conclusion, CD81-targeted UCA allows noninvasive assessment of the expression levels of CD81 on the vascular endothelium and may provide potential insights into early atherosclerotic plaque detection and treatment monitoring.

Keywords

Ultrasound contrast agents; Molecular imaging; CD81; Protein expression; Atherosclerosis

Address correspondence to: Hairong Zheng, PhD., Paul C. Lauterbur Research Center for Biomedical Imaging, Institute of biomedical and Health Engineering, Shenzhen Institutes of Advanced Technology, Chinese Academy of Sciences, Shenzhen, China 518055. hr.zheng@siat.ac.cn.

INTRODUCTION

Noninvasive medical imaging has been made significant advances in the past years. One of the outstanding advances is in the ability to use molecular imaging to assess tissue phenotype (McCarty et al. 2010; Perini et al. 2008), enzymatic activity (Nyati et al. 2010) or protein expression (Lendvai et al. 2009). For target-specific imaging, various modalities, such as ultrasonography (Deshpande et al. 2010), positron emission tomography (Alauddin et al. 2010), magnetic resonance imaging (Sipkins et al. 1998), computed tomography (Li et al. 2010) and optical imaging (Shao et al. 2010), have been applied successfully in preclinical settings. Among these modalities, ultrasound imaging possesses particular attraction due to its high sensitivity, availability, rapid execution of imaging protocols and the relatively low cost (Kaufmann and Lindner 2007). So far, molecular imaging using ultrasound contrast agents (UCA) has been applied to characterize arteriosclerosis (Kaufmann 2009), thrombosis (Alonso et al. 2007), neovasculature (Leong-Poi et al. 2003; Stieger et al. 2008) lymph nodes (Hauff et al. 2004), as well as inflammations (Lindner 2009; Ten Kate et al. 2010). Also, ultrasound molecular imaging has been proven to be highly sensitive to the identification of molecular structures or expression when using targeted contrast agents; thus, it provides helpful insights into genesis, progress and prevention of diseases (Lanza et al. 1996; Lindner 2004; Klibanov 2006; Dayton and Ferrara 2002; Palmowski et al. 2008).

Cluster designation 81 (CD81), a member of the tetraspanin superfamily of cell-surface proteins, tends to associate with integrins, with other tetraspanins and with lineage-specific molecules in the immune system and participates in diverse biologic activities including cell proliferation (Ma et al. 2010), differentiation (Boismenu et al. 1996), adhesion (Levy et al. 1998) and motility (Chambrion and Le Naour 2010; Yáñez-Mó et al. 1998). Recently, through genetic screens, the tetraspanin CD81 was demonstrated to be a marker of early human atherosclerotic plaques (Rohlena et al. 2009). In their study, CD81 was significantly and specifically up-regulated in endothelial cells of atherosclerotic plaques and played a crucial role in the initial stages of atherosclerotic plaque formation. These data indicate that the expression of CD81 proteins in endothelial cells is crucial for genesis and progress of atherosclerosis. In this context, the ability to visualize noninvasively the expression of the marker molecule would be very useful both in preclinical research and in the clinical setting.

Here, we report on the use of antibody-coated gas-filled UCA to target the CD81 in murine endothelial cells that were treated with the phenazine methosulfate (PMS) *in vitro* and *in vivo*. Molecular ultrasound signal enhancement clearly showed that expression of CD81 proteins was significantly up-regulated after PMS stimulation compared with that of untreated controls; the result was also in line with our histologic findings.

MATERIALS AND METHODS

Materials

1,2-distearoyl-sn-glycero-3-phosphatidylcholine (DSPC), 1,2 distearoyl-sn-glycero-3-phosphoethanolamine-N-[Methoxy (Polyethylene glycol)-2000] (DSPE-PEG2000) and 1,2-distearoyl-sn-glycero-3-phosphoethanolamine-N-[Biotinyl(Polyethylene Glycol)2000] (DSPE-PEG2000-Biotin) were purchased from Avanti Polar Lipids Inc. (Alabaster, AL, USA). Avidin, PMS and 4′,6-diamidino-2-phenylindole (DAPI) were obtained from Sigma-Aldrich (St. Louis, MO, USA). Biotinylated anti-CD81 antibody and fluorescein isothiocyanate (FITC)-labeled biotinylated anti-CD81 antibody were purchased from BD Biosciences (San Jose, CA, USA). All other reagents were of analytical grade. Mouse brain microvascular endothelial cells (bEnd.3) were purchased from the American Type Culture

Collection (Manassas, VA, USA). Female BALB/c mice, weighing about 20 g (6–8 weeks old), were obtained from Beijing Weitong Lihua Test Animal Co. (Beijing, China).

Preparation of CD81-targeted UCA

The non-targeted UCA was prepared according to the method we have described previously (Yan et al. 2011). A brush of poly (ethylene glycol) (PEG) was grafted onto the lipid shell, which may prevent the UCA from phagocytosis by macrophage and provide the UCA with longer duration *in vivo*, which may be in favor the accumulation of the target specific UCA (Stieger et al. 2008). Briefly, the DSPC: DSPE-PEG2000: DSPE-PEG2000-biotin with molar ratios (9:0.5:0.5) were added and blended in chloroform. Afterward, the solvent was removed under nitrogen flow at room temperature. The dried phospholipid blends were hydrated at 60°C with 5 mL of phosphate buffer solution (PBS) and perfluoropropane (C_3F_8; Flura, Newport, TN, USA) was added. Finally, the admixture was mechanically vibrated for 45 s to obtain the UCA. The resulting non-targeted UCA ($4.63 \pm 1.51\times10^8$ particles/mL) was used to prepare the CD81-targeted UCA through rinse, incubation of avidin and linkage with biotinylated anti-CD81 antibodies. The FITC-labeled targeted UCA were prepared by using FITC-conjugated biotinylated anti-CD81 antibodies instead of biotinylated anti-CD81 antibodies. Free antibodies were removed by washing with PBS.

Characterization of CD81-targeted UCA

A measurement of 50 μL of FITC-labeled targeted UCA suspension (1×10^8 particles/mL) was applied to the microscope slide. A cover slip was used to cover the sample before the sample was studied under a miscroscope ×400 amplification. Morphologic characteristics of UCA were determined under a fluorescent microscope (Olympus, Tokyo, Japan). Particle size, size distribution and concentration of UCA were determined using an optical particle counter with a 0.5 mm diameter detection limit (Accusizer 780; Particle Sizing Systems, Santa Barbara, CA, USA). For each sample, l00 μL of UCA suspension was analyzed.

Cell culture and *in vitro* induction of CD81 proteins

The murine bEnd.3 endothelial cells (1×10^5 cells/well) were cultured in plates as monolayer in Dulbecco's modified eagles medium (DMEM), supplemented with 10% fetal calf serum and 1% penicillin-streptomycin solution (1% v/v penicillin-streptomycin solution containing 5000 units penicillin and 5 mg streptomycin per mL) and maintained in a humidified atmosphere containing 5% CO_2 at 37°C. To induce expression of CD81 proteins, cells were seeded in 6-well plates overnight to allow cell adhesion. 0, 5, 10 or 20 μL 1 mM of PMS was added into the 1 mL of media (the final concentration is 0, 5, 10 or 20 μM, respectively) and further incubated for 16 h. Cells were collected for Western blot analysis or used for UCA adhesion assay.

Western blot analysis for the expression of CD81 proteins

Stress induced and non-stress induced bEnd.3 cells were lysed in 100 μL ice-cold lysis buffer (Radio-immunoprecipitation assay [RIPA]). The lysates were centrifuged at 12,000 g at 4°C for 5 min and the supernatant was collected. 20 μL of supernatant containing the cell total proteins was separated by 12% sodium dodecyl sulfate polyacrylamide gel electrophoresis (SDS-PAGE) and transferred to polyvinylidene difluouride (PVDF) membranes (Amersham Biosciences, Freiburg, Germany). The PVDF membrane was further incubated with 2 mL PBS solution containing 4 μL Armenian hamster-anti-mouse CD81 primary antibody (0.5 mg/mL, 1:500 dilution; BD Biosciences) and was then incubated with 5 mL PBS solution containing 5 μL goat anti-Armenian hamster IgG HRP-labeled secondary antibody (0.2 mg/mL, 1:1000 dilution; BD Biosciences). The immunoblot was detected using the enhanced chemiluminescence system Super-Signal West Pico

Chemiluminescent Substrate (Pierce, IL, USA). Quantization of CD81 proteins was carried out using Quanti-One software (BioRad, Hercules, CA, USA).

Examination of CD81-targeted UCA binding to bEnd.3 cells

The bEnd.3 cells (1×10^5 cells/well) were seeded in 6-well plates overnight to allow cell adhesion. Cells were stimulated with PMS as stated above. Static binding of CD81-targeted UCA was performed. In brief, 1 mL of 1×10^8 particles/mL CD81-targeted UCA or non-targeted UCA were added into the culture well (media removed) and incubated with the PMS-stress induced bEnd.3 cells or non-stress induced cells for 5 min (gently rotating the plate during the incubation period) and free UCA that did not attach to the cells were removed by a PBS rinse. Then, the number of attached UCA was determined using an optical microscope (Olympus, Tokyo, Japan) at six random fields of view (200 × magnification). As for competitive experiments, 2 μL of 0.5 mg/mL anti-CD81 antibodies were added into the 1 mL media and used to incubate with the stress induced cells for 30 min, followed by examination of CD81-targeted UCA binding.

In vitro imaging of endothelial CD81 expression

bEnd.3 cells (1×10^5 cells/slip) were seeded onto glass cover slips and cultured within a 6-well microplate overnight; 10 μM PMS was added into the media and incubated for 16 h to induce expression of CD81 proteins; and 1×10^8 CD81-targeted UCA were used to adhere to PMS-stress induced cells and non-stress induced cells as stated above. After removing the free UCA with PBS, the cover glass slips attached with cells and UCAwere taken out and insert into a 3% agar phantom side by side. The phantom with the cover slips was placed into a water tank. Then, an ultrasound (US) 60 mm diameter broadband transducer of the responding frequency range 4–15 MHz (Model: L14-5W/60; Ultrasonix Medical Corporation, Richmond, BC, Canada) was positioned at 2 cm distance from the tissue phantom top surface in the axial direction of the ultrasound beam. To prevent the overwhelming specular reflection from the cover glass slips to washout the scattering signal from the sample under examination received by the US transducer, the glass slips were placed tilted at an angle with respect to the US beam axial direction, thus, specular reflected US signals from the cover glass slips could not reach the US transducer (Klibanov et al. 2006). Adhered UCA was detected by SONIX RP ultrasound imaging system (Ultrasonix Medical Corporation, Richmond, BC, Canada). The B-mode images were performed in harmonics mode at 5.0 MHz transmission frequency (depth 2.0 cm, gain: 57%, dynamic range: 75 dB). The difference in mean video intensity (grey-level) between PMS-stimulated cells and non-stimulated cells was calculated using MATLAB (version R2010b; The Mathworks Inc., Natick, MA, USA) and expressed in a box plot.

In vivo studies

All experiments were approved by the review committee of the institution on animal care. As for the stimulated group, a group of BALB/c mice ($n = 5$) were injected by tail vein injection of a dose of 0.25 mg PMS mixed in 100 μL saline per 1 kg body weight to induce expression of CD81 proteins on vascular endothelium. As for control group ($n = 5$), BALB/c mice were not stimulated by tail vein injection of 100 μL saline. After 16 h, both groups of animals were anesthetized by IP injection of pentobarbital sodium (50 mg/kg) and 1×10^7 CD81-targeted UCA (the quantity of UCA was the concentration in microbubbles of the UCA and was suspended in 100 μL of saline) were injected IV into the tail vein catheter. Subsequently, 50 μL of saline were injected to clear the UCA from the catheter.

In vivo image acquisition and quantification

In vivo image acquisition and quantification were made according to the report described in detail by Lyshchik et al. (2007). Briefly, images were acquired with a Vevo770 high-frequency ultrasound system (VisualSonics, Inc., Toronto, Canada), which was equipped with a 40-MHz center frequency transducer. The system was set at 50% transmitting acoustic power with a mechanical index (MI) of 0.14. The ultrasound probe was positioned 2 to 3 mm above the carotid artery. Both the ultrasound probe and the animal were fixed and remained at the same position throughout the study. The dynamic range of the ultrasound scanner was 52 dB. Images were acquired at a 20-Hz frame rate, using 12 mm imaging depth with focused depth at 6 mm. After contrast agent injection, imaging was paused for 3 min to allow binding and retention of the CD81-targeted UCA. After 3 min of waiting period, approximately a sequence of 180 ultrasonographic frames of the carotid artery vessels was acquired at a temporal resolution of 10 s. Subsequently, a high-power ultrasound tone-burst was then applied (20 cycles with a frequency of 10 MHz and a mechanical index of 0.59) to destroy bubbles. After the bubble-destruction pulse, the system was reset with identical imaging parameters as before the destruction event and another set of images (≈180 frames) was then acquired.

Image processing and quantification were performed with the software implemented in the ultrasound scanner, relying on two sets of images: a pre-destruction set and a post-destruction (background) data set. To determine signal from retained UCA, images from the pre-destruction set were paired to their partner images in the post-destruction set (Lyshchik et al. 2007). The post-destruction imaging signals were subtracted from the pre-destruction imaging signal. The resulting imaging signals, which provide a map of the spatial distribution of the UCA retained by the tissue, were displayed in shades of green. The mean video intensity of pre-destruction and post-destruction sonograms was measured in a region-of-interest encompassing the examined vessels (about 1.20 mm^2). The difference in video intensity between pre-destruction and post-destruction ultrasonographic frames was calculated and expressed in a box plot. This value provided a relative measure of the amount of the CD81-targeted UCA retained by the vessels.

Immunohistochemistry

Immediately following final imaging, the carotid artery samples were dissected for histologic phenotyping, covered with Tissue-Tek (Sakura, Torrance, CA, USA), and then frozen in liquid nitrogen vapor. The carotid artery sections (6 μm thick) were cut with a cryostat microtome (CM1950; Leica, Heidelberg, Germany). Double immunostaining was done using 1 μL Armenian hamster anti-mouse CD81 antibody (0.5 mg/mL, 1:50 dilution in PBS; BD Biosciences) and 1 μL secondary antibody, FITC-labeled rabbit anti-Armenian hamster IgG (0.1 mg/mL 1:100 dilution in PBS; BD Biosciences). Cell nuclei were counterstained by 4′,6-diamidino-2-phenylindole (1:100 dilution in PBS; Invitrogen). Tissue fluorescence sections were viewed under a confocal microscope (Olympus FV1000 confocal microscope; Olympus, Tokyo, Japan). The mean fluorescent intensity of veins was quantitatively evaluated by Image J software (National Institutes of Health, Bethesda, MD, USA).

Statistical evaluation

Data are presented as mean values of N trials (N ≥3) unless otherwise stated. Statistical analysis for bubble size, protein expression and attachment number of bubbles with cells was performed using two-tailed *t*-test assuming unequal variances. Video intensity of contrast-enhanced sonograms was presented as median (IQR) and analyzed with the Mann-Whitney test ($p < 0.05$ and $p < 0.01$ were considered to show significant and highly significant differences, respectively).

RESULTS

Characterization of the CD81-targeted UCA

Figure 1a showed the surface of the fluorescent-labeled CD81-targeted UCA appeared green under fluorescent microscope, which indicated the successful conjugation of anti-CD81 antibodies to the surface of UCA when FITC-labeled biotinylated anti-CD81 antibodies were used to replace for biotinylated anti-CD81 antibodies. Typical size distributions of non-targeted and CD81-targeted UCA are shown in Figure 1b. The size distribution for CD81-targeted UCA was centered at ~0.88 μm diameter with secondary peaks at ~3.22 and ~6.49 μm diameters, with a slight different distribution for non-targeted UCA, which was centered at ~0.71 μm diameter with secondary peaks at 33.40 and ~6.85 μm diameter.

CD81 expression detection

Rohlena et al. (2009) reported that CD81 proteins can be induced by phenazine methosulfate (PMS) and resulted in up-regulation of CD81 expression on the mRNA, as well as the protein level. We next examined the dose effect on expression of CD81 proteins in response to the oxidative stress inducer PMS. Results showed CD81 was only faintly detected in Western blots in non-stress induced bEnd.3 cells. In contrast, incubation of bEnd.3 with 5, 10 and 20 μM of PMS for 16 h caused a dose-dependent increase in CD81 expression (Fig. 2a). Quantization of CD81 proteins is shown in Figure 2b. There were, respectively, 1.56, 1.94 and 2.71-fold increases in CD81 expression following the corresponding 5, 10 and 20 μM of PMS treatments, compared with those of untreated controls ($p < 0.01$).

Examination of CD81-targeted UCA binding affinity to bEnd.3 cells

To examine binding affinity and specificity, CD81-targeted UCA or non-targeted UCA were incubated with PMS-stress induced bEnd.3 cells. Results showed there was rarely binding of non-targeted UCA to stress induced bEnd.3 cells. In contrast, a large number of CD81-targeted UCA were found to be bound to the surface of stress induced bEnd.3 cells (Fig. 3a). There were only 111 ± 21 UCA bound to the non-stress induced cells per view field, while 336 ± 46, 634 ± 32, 760 ± 43 UCA bound to the stress induced cells when using 5, 10, 20 μM of PMS treatment, respectively ($p < 0.01$) (Fig. 3b). Interestingly, the binding of UCA to stress induced cells could be inhibited dramatically, with the result of 56 ± 12 UCA bound to 10 μM PMS-stimulated cells, which were blocked by free anti-CD81 antibodies ($p < 0.05$). Thus, the number of CD81-targeted UCA was gradually improved with increase of PMS concentration and could be inhibited considerably, which further proved the specific attachment of targeted UCA with cells.

In vitro molecular imaging via CD81-targeted UCA

To examine whether CD81-targeted UCA were able to detect the expression of CD81 proteins, stress induced or non-stress induced bEnd.3 cells were incubated with the CD81-targeted UCA and imaged by ultrasound imaging system (Fig. 4a). Figure 4b demonstrated that the ultrasonic signals of 10 μM PMS stress induced cells bound with CD81-targeted UCA was significantly enhanced (Fig. 4b, left), while the non-stress induced cells showed faint signals due to the weak adhesion of UCA (Fig. 4b, right). The quantitative gray-level of the images of the stress induced and non-stress induced cells was shown in Figure 4c. The mean gray-level was 17.2 (IQR, 15.4–19.8) for stress induced cells, significantly higher than that of non-stress induced cells with 9.0 (IQR, 8.6–10.8) ($p < 0.01$).

In vivo molecular imaging via CD81-targeted UCA

To further examine the application of the CD81-targeted UCA to the effect of imaging the expression of CD81 proteins *in vivo*, the carotid artery vessels of the PMS-stimulated and

non-stimulated mice were examined. Figure 5 showed representative images of the PMS-stimulated and non-stimulated carotid artery vessels with the CD81-targeted UCA. Similar to *in vitro* imaging results, there was evident enhancement (green signals) in the ultrasound signal from the CD81-targeted UCA retained in the PMS-stimulated vessel walls (Fig. 5a). Only a weak signal of UCA was detected in the non-stimulated vessel walls, compared with that of the stimulated vessel walls, (Fig. 5b). Quantitative analysis of the sonograms showed that the mean video intensity was significantly increased, with 27.2 (IQR, 22.4–29.8) for the stimulated vessels vs. 11.3 (IQR, 10.4–13.2) for the non-stimulated control (Fig. 5c, $p < 0.01$).

Immunofluorescence assay

To validate the results of ultrasonography, the carotid artery of mice were harvested and subsequently analyzed for CD81 expression by immunofluorescence assay. Results showed consistently greater levels of CD81 in the endothelium of carotid artery vessel wall, compared with that of non-stimulated endothelium of the arterial wall (Fig. 6, arrow). The quantitative analysis showed the mean fluorescent intensity is 13.57 ± 1.20, significantly higher than that of the non-stimulated vessels with 7.11 ± 0.41 ($p < 0.01$). It demonstrated the result of histologic evaluation of endothelial cells of carotid artery vessels was correlated well with the ultrasound signal enhancement obtained with the CD81-targeted UCA.

DISCUSSION

Atherosclerosis is a systemic disease, characterized by lipid deposition, leukocyte infiltration and intimal thickening, which affects most major arteries of the body and is the most common cause of premature people death in the western world (Lusis 2000; Davies et al. 2004). Given the fact that atherosclerosis is a complex, chronic disorder involving inflammatory and proliferative signaling pathways, it is especially important to identify and quantify the specific molecular markers of atherosclerosis to provide diagnostic and prognostic information and to establish a basis for early atherosclerosis treatment response evaluation. According to the Rohlena's finding, the expression pattern of endothelial cell CD81 is an ideal molecular marker for evaluating the atherosclerosis prior to the full-blown inflammatory response (Rohlena et al. 2009), which triggered us to investigate the feasibility for visualizing noninvasively the expression of the marker molecule using targeted ultrasound contrast agents.

Phenazine methosulphate (PMS) is a strong oxidant that induces reactive oxygen species (ROS) formation in cells. In the vasculature, increased ROS production has been associated with endothelial dysfunction, an early pathogenic event in atherosclerosis (Wang et al. 2000). In our study, it has been shown that a dose-dependent manner of CD81 expression after PMS treatment, which agrees with Rohlena's results (Rohlena et al. 2009).

Western blotting and immunocytochemistry staining are the most popular approaches to detect expression of proteins in the preclinical animals or clinic patients. Both need to collect *ex vivo* samples from animals or patients. Usually, invasive surgeries have to be performed and a set of experiment procedures have to be followed. In some cases, it is difficult to collect samples, particularly for patients with cardiovascular disease. In comparison, although ultrasound imaging with UCA still has room to improve, it has some advantages in preclinical applications, such as that it is readily available, easy to use and has the fast response-time to provide real-time imaging. More importantly, ultrasound imaging uses contrast agents that remain exclusively intravascular, minimizing nonspecific signals from extravasated contrast material. Our results indicated that the intensity of the ultrasound signal from the bound CD81-targeted UCA correlates well with relative expression of CD81 by immunoblotting or immunocytochemistry. Although these data may not be directly

comparable, these findings are especially valuable since imaging can provide an alternative strategy for evaluating early response to oxidant stress stimulation in terms of spatial extent and amount of endothelial CD81 proteins in a noninvasive or minimal-invasive manner. In fact, numerous investigators have adopted approaches in which molecular imaging has been attained through the use of targeted gas-filled UCA and many proteins related to atherosclerosis such as ICAM-1 (Demos et al. 1999) VCAM-1 (Hamilton et al. 2004) P-selectin (Lindner et al. 2001) von Willebrand factor (McCarty et al. 2010) (vWF) and integrins (Leong-Poi et al. 2003), have been imaged with targeted ultrasound probes.

In this work, avidin-biotin adhesion was employed between anti-CD81 antibodies and UCA, given the fact that the strongest known non-covalent interaction between a protein and a ligand with an affinity of 10^{15} M^{-1} at pH 5. It was found by Kheirolomoom et al. (2007) that by using (strept) avidin bridge, UCA can be easily decorated with a wide variety of ligands or combinations of ligands. The distribution of both targeted UCA and non-targeted UCA has some multiple peaks. There is a slightly greater size at the centered diameter for the target-specific UCA than that of non-targeting UCA. The distribution of multiple peaks founded is similar with that of Borden' report (Borden et al. 2008) and the slightly greater size at centered diameter possibly results from the surface architectures.

In our study, the carotid artery vessels were particularly selected as target-region to examine the ultrasonography from the target-specific UCA *in vivo*. Reasons mainly result from the following facts. First, the carotid artery vessels are readily accessible and detected under ultrasound imaging systems. Second, vascular endothelium is easier to expose to the PMS inducers and more sensitively up-regulated for the expression of CD81 proteins. Third, only intravascular targets, especially expressed on the surface of vascular endothelium can be targeted with these agents since UCA rarely extravagates from the vasculature owing to their relatively large size. More importantly, the carotid and subclavian arteries are often the first involved vessels in atherosclerosis (Rigatelli and Zanchetta 2005). Although targeting with ultrasound contrast agents for molecular imaging of large arteries is still a challenge due to the high shear stress, our results has shown anti-CD81-coated UCA enables molecular imaging of CD81 expression onvascular endothelium. Our success may be contribute to the relatively small size of UCA (about 0.88 μm with centered diameter distribution) and high level expression of CD81 proteins with four transmembrane (TM) helices. Indeed, it was demonstrated that a small size favors attachment of targeted UCA at high shear stresses. With decreasing diameter, the shear stress required to set a particle in motion becomes higher (Shinde Patil et al. 2001). Moreover, CD81 is an expressed cell-surface protein, which plays in an important role in adhesion (Levy et al. 1998). The crystal structure of human CD81 large cysteine-rich extracellular domain demonstrated each subunit within the homodimeric protein displays a mushroom-like structure, composed of five-helices arranged in "stalk" and "head" subdomains. These structural characteristics make it more easily form firm adhesion with anti-CD81 antibodies (Higginbottom et al. 2000; Petracca et al. 2000; Kitadokoro et al. 2001).

In this study, we used two different imaging systems with different frequencies and obtained different maps for imaging *in vitro* and *in vivo*. Although those data are taken using two different imaging systems, the data obtained from the same imaging systems *in vitro* or *in vivo* are still comparable. They can provide a relative gray-level of the signal intensity. In *in vitro* imaging experiment, it is notable that the time needed to make the *in vitro* measurements must be as short as possible because some bubbles may have dissolved during this time. In *in vivo* imaging experiment, images were collected before and shortly after a destructive pulse. The imaging signals (grey-level) from these 180 imaging frames were averaged and digitally subtracted from the initial 180 (pre-destruction) frames to minimize the effects from slight tissue motion artifacts. The resulting differences in grey-level

corresponded to the imaging signal were displayed to provide a map of the spatial distribution of UCA adhering to endothelial cell molecular markers. It is reasonable to assume that the UCA concentration in the blood is comparable before and after the destructive pulse since the disturbance of US was very minimal, thus, the grey-level difference represents the contribution of the scattering from the bound UCA. In fact, the B-mode ultrasound imaging protocol and the grey-level quantification used to detect retention of targeted UCA have been widely accepted and applied in ultrasound molecular imaging (Stieger et al. 2008; Lyshchik et al. 2007; Kiessling et al. 2011).

There are several limitations of this study. First, for the preparation of targeted UCA, biotin binds to avidin in a non-covalent and very stable manner by which biotinylated antibodies or peptides can then be linked to the UCA. However, this strategy is not translatable since avidin is immunogenic in humans from the clinical perspective. Second, it cannot be assumed that the models we used to test the feasibility of CD81-targeted UCA are identical to disease-related CD81 expression. In the clinical setting, more complex factors such as disease-related inducers, individual differences and intricate signal pathway are often involved into the regulation of CD81 expression. Although there is still a long way to translate this technique from the animal model to the clinical situation, it is eventually desirable to couple the level of video-intensity signal from the targeted microbubbles to the stage of the disease and to the risk assessment of atherosclerosis. Due to there is high patient to patient variation, it will be necessary to image besides the effected carotid artery or a control artery, in which the expression of CD81 must be less. Third, precise spatial correlation between ultrasonography and immunohistology was not possible due to the difficulty of spatially matching the ultrasound plane with histologic sections and the fact 2-dimensional ultrasonography is formed from signals received over a beam elevation of several millimeters (Leong-Poi et al. 2003). Fourth, the accuracy of CD81 quantification using the targeted UCA may be limited by some degree of nonspecific binding due to the wide and overlapping expression of CD81 by the vascular endothelium. In addition, it should also be noted that the increase in the difference signal in green only showed on one side of the vessel, while no UCA attached to the other side, which indicates that more complex factors, such as acoustic radiation force, UCA concentration, blood flow velocity and targeted UCA affinity are involved and need to be further investigated. Indeed, acoustic radiation force can push the UCA forward to the side of the vessel and enhance the adhesion of targeted UCA to the endothelial cells (Zhao et al. 2004). Therefore, future studies including examination of the feasibility for assessing atherosclerosis and optimization of relative parameters using the CD81-targeted UCA are required.

CONCLUSIONS

This study demonstrated the successful preparation of the CD81-targeted UCA and the potential of target-specific UCA to detect the increased expression of CD81 proteins stress induced by PMS stimulation *in vitro* and *in vivo*. Our initial experience in molecular ultrasonography using the CD81-targeted UCA has shown that it may enable *in vitro* and *in vivo* molecular imaging of CD81 expression on vascular endothelium. This imaging modality may provide reference values of relative expression of CD81 and information likely to be very useful to address the detection, prognosis, vulnerable potential of atherosclerosis or susceptibility to anti-atherosclerosis drugs.

Acknowledgments

This work is supported by National Basic Research Program 973 (Grant Nos. 2010CB732604, 2011CB707903 and 2010CB534914) from Ministry of Science and Technology, China, National Science Foundation Grants (Grant Nos. 81027006, 61020106008, 10904094, 10904095, 30900749, 30970833, 11002152 and 61002001), 2010-

Guangdong Innovational Research Team Program, Shenzhen Basic Research Program (Grant No. JC201005280495A) and Shenzhen-Hong Kong Innovation Circle Grant.

References

Alauddin MM, Gelovani JG. Radiolabeled nucleoside analogues for PET imaging of HSV1-tk gene expression. Curr Top Med Chem. 2010; 10:1617–1632. [PubMed: 20583993]

Alonso A, Della Martina A, Stroick M, Fatar M, Griebe M, Pochon S, Schneider M, Hennerici M, Allémann E, Meairs S. Molecular imaging of human thrombus with novel abciximab immunobubbles and ultrasound. Stroke. 2007; 38:1508–1514. [PubMed: 17379828]

Boismenu R, Rhein M, Fischer WH, Havran WL. A role for CD81 in early T cell development. Science. 1996; 271:198–200. [PubMed: 8539618]

Borden MA, Zhang H, Gillies RJ, Dayton PA, Ferrara KW. A stimulus-responsive contrast agent for ultrasound molecular imaging. Biomaterials. 2008; 29:597–606. [PubMed: 17977595]

Chambrion C, Le Naour F. The tetraspanins CD9 and CD81 regulate CD9P1-induced effects on cell migration. PLoS One. 2010; 5:e11219. [PubMed: 20574531]

Davies JR, Rudd JH, Weissberg PL. Molecular and metabolic imaging of atherosclerosis. J Nucl Med. 2004; 45:1898–1907. [PubMed: 15534061]

Dayton PA, Ferrara KW. Targeted imaging using ultrasound. J Magn Reson Imaging. 2002; 16:362–377. [PubMed: 12353252]

Demos SM, Alkan-Onyuksel H, Kane BJ, Ramani K, Nagaraj A, Greene R, Klegerman M, McPherson DD. *In vivo* targeting of acoustically reflective liposomes for intravascular and transvascular ultrasonic enhancement. J Am Coll Cardiol. 1999; 33:867–875. [PubMed: 10080492]

Deshpande N, Needles A, Willmann JK. Molecular ultrasound imaging: Current status and future directions. Clin Radiol. 2010; 65:567–581. [PubMed: 20541656]

Hamilton AJ, Huang S-L, Warnick D, Rabbat M, Kane B, Nagaraj A, Klegerman M, McPherson DD. Intravascular ultrasound molecular imaging of atheroma components in vivo. J Am Coll Cardiol. 2004; 43:453–460. [PubMed: 15013130]

Hauff P, Reinhardt M, Briel A, Debus N, Schirner M. Molecular targeting of lymph nodes with L-selectin ligand-specific US contrast agent: A feasibility study in mice and dogs. Radiology. 2004; 231:667–673. [PubMed: 15118116]

Higginbottom A, Quinn ER, Kuo CC, Flint M, Wilson LH, Bianchi E, Nicosia A, Monk PN, McKeating JA, Levy S. Identification of amino acid residues in CD81 critical for interaction with hepatitis C virus envelope glycoprotein E2. J Virol. 2000; 74:3642–3649. [PubMed: 10729140]

Kaufmann BA, Lindner JR. Molecular imaging with targeted contrast ultrasound. Curr Opin Biotechnol. 2007; 18:11–16. [PubMed: 17241779]

Kaufmann BA. Ultrasound molecular imaging of atherosclerosis. Cardiovasc Res. 2009; 83:617–625. [PubMed: 19493955]

Kheirolomoom A, Dayton PA, Lum AF, Little E, Paoli EE, Zheng H, Ferrara KW. Acoustically-active microbubbles conjugated to liposomes: Characterization of a proposed drug delivery vehicle. J Control Release. 2007; 118:275–284. [PubMed: 17300849]

Kiessling F, Gaetjens J, Palmowski M. Application of molecular ultrasound for imaging integrin expression. Theranostics. 2011; 1:127–134. [PubMed: 21547155]

Kitadokoro K, Bordo D, Galli G, Petracca R, Falugi F, Abrignani S, Grandi G, Bolognesi M. CD81 extracellular domain 3D structure: Insight into the tetraspanin superfamily structural motifs. EMBO J. 2001; 20:12–18. [PubMed: 11226150]

Klibanov AL, Rychak JJ, Yang WC, Alikhani S, Li B, Acton S, Lindner JR, Ley K, Kaul S. Targeted ultrasound contrast agent for molecular imaging of inflammation in high-shear flow. Contrast Media Mol Imaging. 2006; 1:259–266. [PubMed: 17191766]

Klibanov AL. Microbubble contrast agents: Targeted ultrasound imaging and ultrasound-assisted drug-delivery applications. Invest Radiol. 2006; 41:354–362. [PubMed: 16481920]

Lanza GM, Wallace KD, Scott MJ, Cacheris WP, Abendschein DR, Christy DH, Sharkey AM, Miller JG, Gaffney PJ, Wickline SA. A novel site-targeted ultrasonic contrast agent with broad biomedical application. Circulation. 1996; 94:3334–3340. [PubMed: 8989148]

Lendvai G, Estrada S, Bergstrom M. Radiolabelled oligonucleotides for imaging of gene expression with PET. Curr Med Chem. 2009; 16:4445–4461. [PubMed: 19835563]

Leong-Poi H, Christiansen J, Klibanov AL, Kaul S, Lindner JR. Nonin-vasive assessment of angiogenesis by ultrasound and microbubbles targeted to alpha (v)-integrins. Circulation. 2003; 107:455–460. [PubMed: 12551871]

Levy S, Todd SC, Maecker HT. CD81 (TAPA-1): A molecule involved in signal transduction and cell adhesion in the immune system. Annu Rev Immunol. 1998; 16:89–109. [PubMed: 9597125]

Li J, Chaudhary A, Chmura SJ, Pelizzari C, Rajh T, Wietholt C, Kurtoglu M, Aydogan B. A novel functional CT contrast agent for molecular imaging of cancer. Phys Med Biol. 2010; 55:4389–4397. [PubMed: 20647599]

Lindner JR, Song J, Christiansen J, Klibanov AL, Xu F, Ley K. Ultrasound assessment of inflammation and renal tissue injury with microbubbles targeted to P-selectin. Circulation. 2001; 104:2107–2112. [PubMed: 11673354]

Lindner JR. Contrast ultrasound molecular imaging of inflammation in cardiovascular disease. Cardiovasc Res. 2009; 84:182–189. [PubMed: 19783842]

Lindner JR. Microbubbles in medical imaging: Current applications and future directions. Nat Rev Drug Discov. 2004; 3:527–532. [PubMed: 15173842]

Lusis AJ. Atherosclerosis. Nature. 2000; 407:233–241. [PubMed: 11001066]

Lyshchik A, Fleischer AC, Huamani J, Hallahan DE, Brissova M, Gore JC. Molecular imaging of vascular endothelial growth factor receptor 2 expression using targeted contrast-enhanced high-frequency ultrasonography. J Ultrasound Med. 2007; 26:1575–1586. [PubMed: 17957052]

Ma J, Liu R, Peng H, Zhou J, Li H. CD81 inhibits the proliferation of astrocytes by inducing G(0)/G(1) arrest *in vitro*. J Huazhong Univ Sci Technolog Med Sci. 2010; 30:201–205. [PubMed: 20407874]

McCarty OJ, Conley RB, Shentu W, Tormoen GW, Zha D, Xie A, Qi Y, Zhao Y, Carr C, Belcik T, Keene DR, de Groot PG, Lindner JR. Molecular imaging of activated von Willebrand factor to detect high-risk atherosclerotic phenotype. JACC Cardiovasc Imaging. 2010; 3:947–955. [PubMed: 20846630]

Nyati S, Ross BD, Rehemtulla A, Bhojani MS. Novel molecular imaging platform for monitoring oncological kinases. Cancer Cell Int. 2010; 10:23. [PubMed: 20615241]

Palmowski M, Huppert J, Ladewig G, Hauff P, Reinhardt M, Mueller MM, Woenne EC, Jenne JW, Maurer M, Kauffmann GW, Semmler W, Kiessling F. Molecular profiling of angiogenesis with targeted ultrasound imaging: Early assessment of antiangiogenic therapy effects. Mol Cancer Ther. 2008; 7:101–109. [PubMed: 18202013]

Perini R, Pryma D, Divgi C. Molecular imaging of renal cell carcinoma. Urol Clin North Am. 2008; 35:605–611. [PubMed: 18992614]

Petracca R, Falugi F, Galli G, Norais N, Rosa D, Campagnoli S, Burgio V, Di Stasio E, Giardina B, Houghton M, Abrignani S, Grandi G. Structure-function analysis of hepatitis C virus envelope-CD81 binding. J Virol. 2000; 74:4824–4830. [PubMed: 10775621]

Rigatelli G, Zanchetta M. Endovascular therapies for noncoronary atherosclerosis in the elderly: Supra-aortic vessels and thoraco abdominal aorta lesions. Am J Geriatr Cardiol. 2005; 14:142–147. [PubMed: 15886540]

Rohlena J, Volger OL, van Buul JD, Hekking LH, van Gils JM, Bonta PI, Fontijn RD, Post JA, Hordijk PL, Horrevoets AJ. Endothelial CD81 is a marker of early human atherosclerotic plaques and facilitates monocyte adhesion. Cardiovasc Res. 2009; 81:187–196. [PubMed: 18805782]

Shao Q, Xing B. Photoactive molecules for applications in molecular imaging and cell biology. Chem Soc Rev. 2010; 39:2835–2846. [PubMed: 20480074]

Shinde Patil VR, Campbell CJ, Yun YH, Slack SM, Goetz DJ. Particle diameter influences adhesion under flow. Biophys J. 2001; 81:187–196.

Sipkins DA, Cheresh DA, Kazemi MR, Nevin LM, Bednarski MD, Li KC. Detection of tumor angiogenesis *in vivo* by alphaVbeta3-targeted magnetic resonance imaging. Nat Med. 1998; 4:623–626. [PubMed: 9585240]

Stieger SM, Dayton PA, Borden MA, Caskey CF, Griffey SM, Wisner ER, Ferrara KW. Imaging of angiogenesis using Cadence contrast pulse sequencing and targeted contrast agents. Contrast Media Mol Imaging. 2008; 3:9–18. [PubMed: 18335479]

Ten Kate GL, Sijbrands EJ, Valkema R, ten Cate FJ, Feinstein SB, van der Steen AF, Daemen MJ, Schinkel AF. Molecular imaging of inflammation and intraplaque vasa vasorum: A step forward to identification of vulnerable plaques? J Nucl Cardiol. 2010; 17:897–912. [PubMed: 20552308]

Wang W, Wang S, Yan L, Madara P, Del Pilar Cintron A, Wesley RA, Danner RL. Superoxide production and reactive oxygen species signaling by endothelial nitric-oxide synthase. J Biol Chem. 2000; 275:16899–16903. [PubMed: 10747895]

Yan F, Li X, Jin Q, Jiang C, Zhang Z, Ling T, Qiu B, Zheng H. Therapeutic ultrasonic microbubbles carrying paclitaxel and LyP-1 peptide: Preparation, characterization and application to ultrasound assisted chemotherapy in breast cancer cells. Ultrasound Med Biol. 2011; 37:768–779. [PubMed: 21458148]

Yáñez-Mó M, Alfranca A, Cabañnas C, Marazuela M, Tejedor R, Ursa MA, Ashman LK, de Landázuri MO, Sánchez-Madrid F. Regulation of endothelial cell motility by complexes of tetraspan molecules CD81/TAPA-1 and CD151/PETA-3 with alpha3 beta1 integrin localized at endothelial lateral junctions. J Cell Biol. 1998; 141:791–804. [PubMed: 9566977]

Zhao S, Borden M, Bloch SH, Kruse D, Ferrara KW, Dayton PA. Radiation-force assisted targeting facilitates ultrasonic molecular imaging. Mol Imaging. 2004; 3:135–148. [PubMed: 15530249]

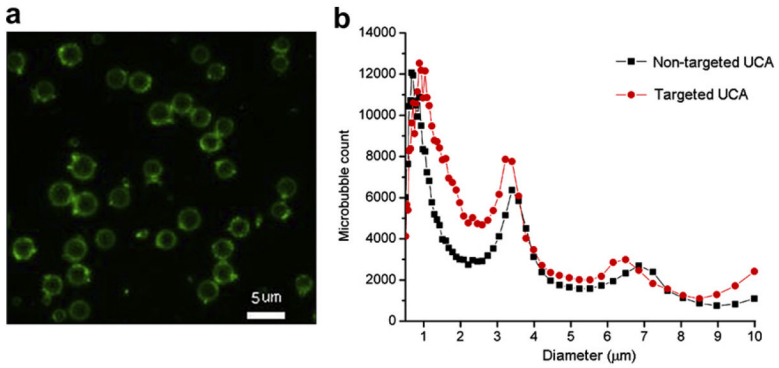

Fig. 1.

Characterization of the CD81-targeted ultrasound contrast agents. (a) Fluorescent micrograph of fluorescein iso-thiocyanate (FITC)-labeled CD81-targeted ultrasound contrast agents (UCA) (bar = 5 μm). (b) Size distribution of the targeted UCA and non-targeted UCA.

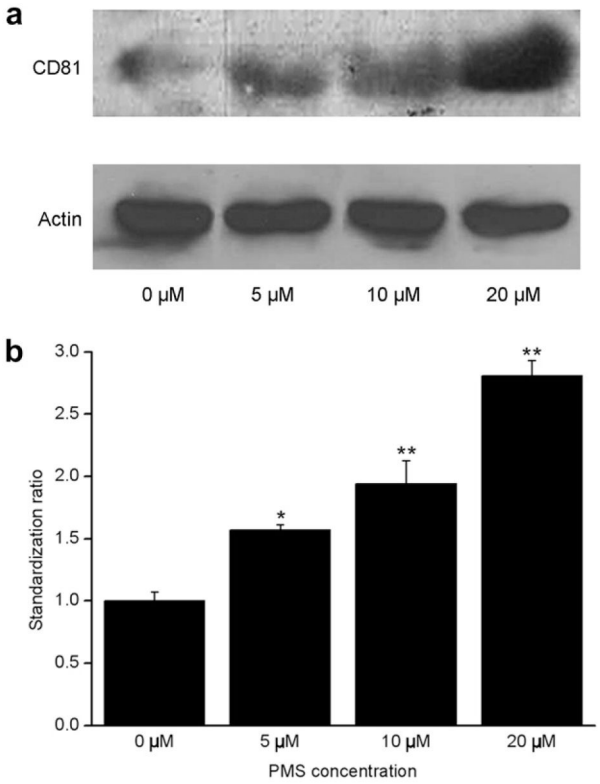

Fig. 2.

Immunoblotting for CD81 expression in bEnd.3 cells. (a) Immunoblotting assay for CD81 proteins extracted from bEnd.3 cells, which were incubated with 0, 5, 10 and 20 μM of phenazine methosulfate (PMS) for 16 h and from untreated control. The top row stands for CD81 proteins, indicating a gradual increasing trend with the increase of PMS concentrations. The bottom row stands for beta-actins that served here as a loading control and were kept constantly. (b) Quantitative assay of CD81 proteins through Quanti-One software. ** $p < 0.01$ (n = 3).

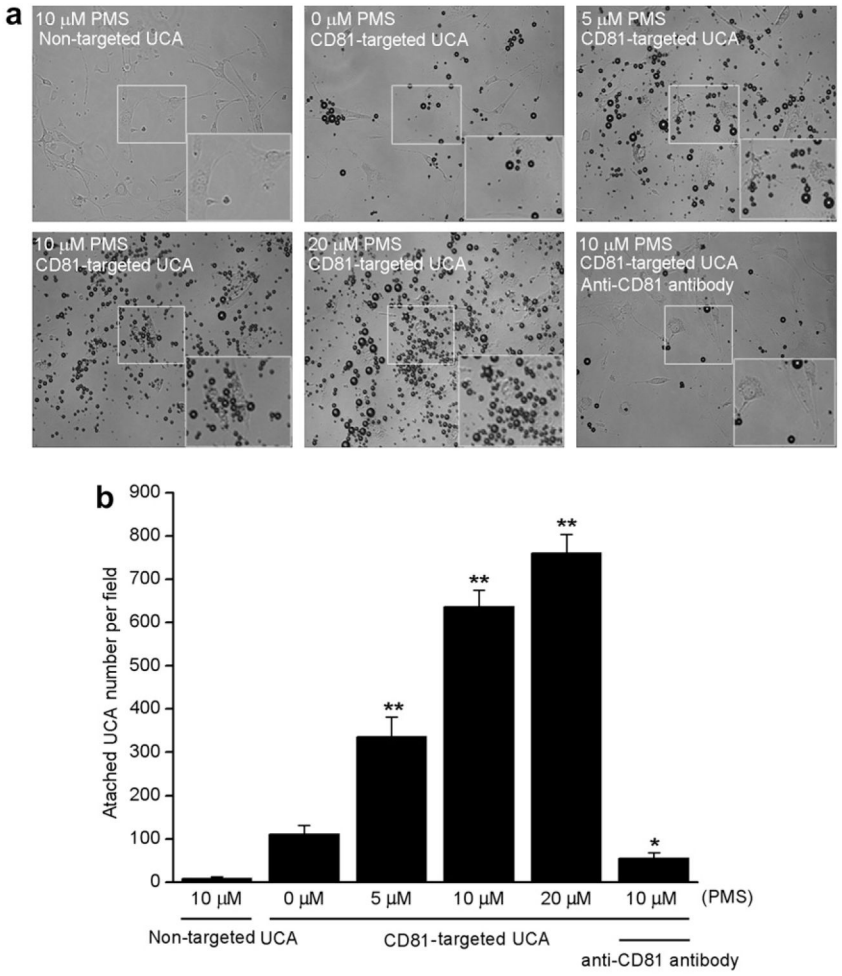

Fig. 3.

CD81-targeted ultrasound contrast agents (UCA) binding to cultured bEnd.3 cells. (a) Representative micrograph for CD81-targeted UCA or non-targeted UCA adhered to cells stimulated with 0, 5, 10 or 20 μM phenazine methosulfate (PMS)(×200). Non-targeted UCA was not able to bind to the cells stimulated with 10 μM PMS (top left). Just a few CD81-targeted UCA was able to bind to the cells without PMS stimulation (top middle). The number of CD81-targeted UCA was gradually improved with increase of PMS concentration from 5 μM (top right), 10 μM (bottom left) to 20 μM (bottom middle). Pre-incubation using 1 μg/mL free anti-CD81 antibodies with 10 μM PMS-stimulated cells inhibited greatly the binding of CD81-targeted UCA to the cells (bottom right). The boxes located the center of pictures stand for the selected regions amplified for making the cells more visible. The boxes located the bottom right of pictures stand for the amplified view of the selected regions. (b) Quantitative assay of the number of UCA adhered onto bEnd.3 cells from six at random view field. * $p < 0.05$ and ** $p < 0.01$ vs non-stimulation control (n = 6).

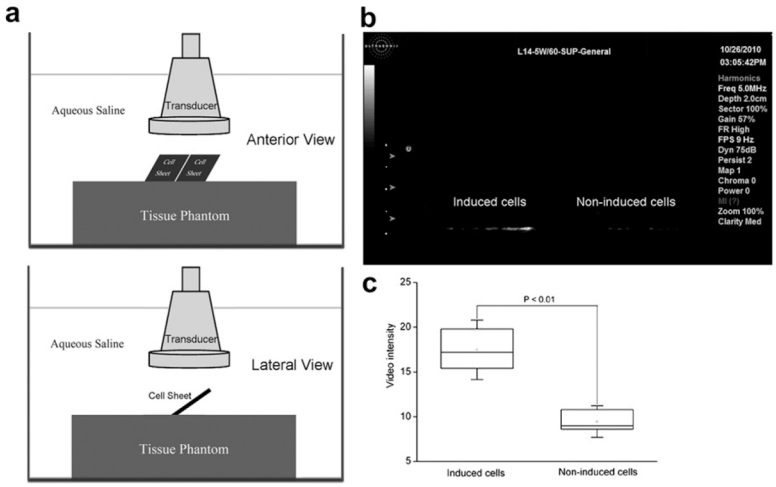

Fig. 4.

Ultrasound molecular imaging of CD81 expression *in vitro*. (a) Schematic diagram of *in vitro* ultrasound molecular imaging of CD81 expression (Top: anterior view, Bottom: lateral view). (b) B-mode ultrasound imaging to detect the CD81 expression *via* CD81-targeted ultrasound contrast agents (UCA) adhered to the stress induced (right) and non-stress induced (left) cells, which were cultivated on 20 mm glass cover slides inserted into the phantom. Imaging was performed with an SONIX RP ultrasound imaging system. (c) Box plot of the gray-level of the B-mode images for the stress induced and non-stress induced bEnd.3 cells.

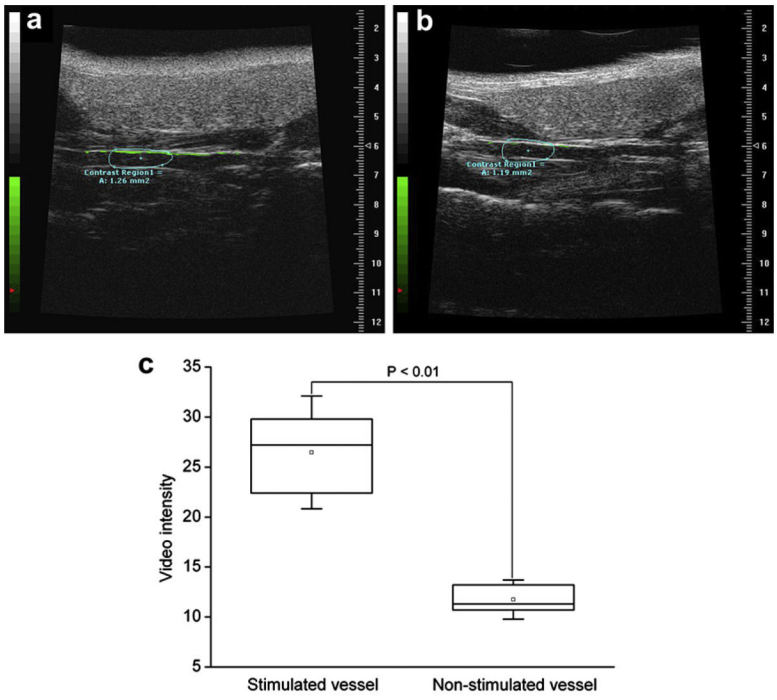

Fig. 5.

Molecular sonograms of carotid artery vessels. (a) Ultrasound imaging to detect the CD81 expression for the phenazine methosulfate (PMS)-stimulated vessels. (b) Ultrasound imaging to detect the CD81 expression for the non-stimulated vessels. Molecular imaging signal from attached ultrasound contrast agents (UCA) was color coded as green signals overlaid on gray-scale ultrasound image. There was a great enhancement in the ultrasound signal from the CD81-targeted UCA retained in the PMS-stimulated vessel wall, compared with the non-stimulated vessel wall. (c) Box plot of video intensity for the stimulated and non-stimulated carotid artery vessels. The selected contrast regions were marked with boxes.

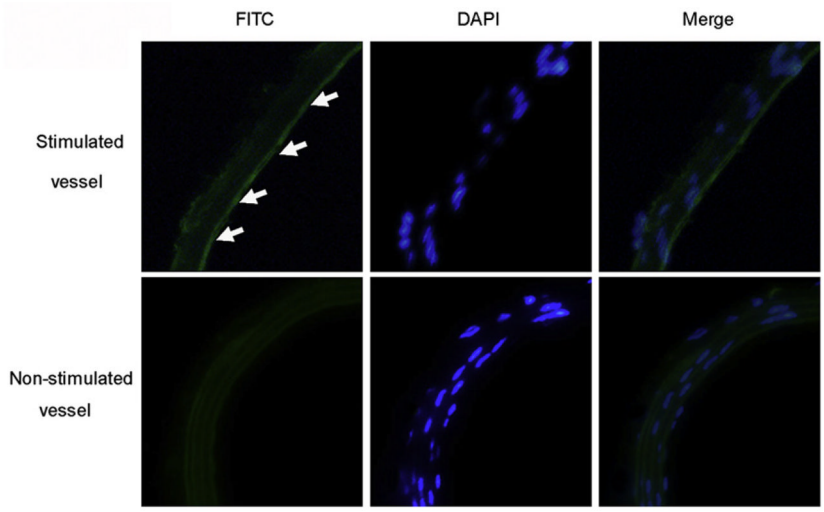

Fig. 6.

Immunofluorescence assay for CD81 expression on the carotid artery section. Representative confocal micrographs from the stimulated and non-stimulated carotid artery vessels incubated with fluorescein isothiocyanate (FITC)-labeled anti-CD81 antibodies appear green (left column). The nuclei were stained by 4′,6-diamidino-2-phenylindole (DAPI) and showed blue (middle column). The overlaying images were obtained by FITC filter and DAPI filter (right column). In comparison, a significant higher expression level of CD81 was observed from the stimulated carotid artery vessel wall (arrow) than that of non-stimulated vessel wall (×200).